Letter

Impact of chaos on precursors of quantum criticality

Ignacio García-Mata,[1] Eduardo Vergini,[2,3] and Diego A. Wisniacki[4]

[1]*Instituto de Investigaciones Físicas de Mar del Plata, Facultad de Ciencias Exactas y Naturales, Universidad Nacional de Mar del Plata and CONICET, 7600 Mar del Plata, Argentina*

[2]*Departamento de Física, Comisión Nacional de Energía Atómica, Avenida del Libertador 8250, (C1429BNP) Buenos Aires, Argentina*

[3]*Escuela de Ciencia y Tecnología, Universidad Nacional de General San Martín, Alem 3901, (B1653HIM) Villa Ballester, Argentina*

[4]*Departamento de Física "J. J. Giambiagi" and IFIBA, FCEyN, Universidad de Buenos Aires, 1428 Buenos Aires, Argentina*

(Received 14 April 2021; revised 1 June 2021; accepted 9 December 2021; published 27 December 2021)

Excited-state quantum phase transitions (ESQPTs) are critical phenomena that generate singularities in the spectrum of quantum systems. For systems with a classical counterpart, these phenomena have their origin in the classical limit when the separatrix of an unstable periodic orbit divides phase space into different regions. Using a semiclassical theory of wave propagation based on the manifolds of unstable periodic orbits, we describe the quantum states associated with an ESQPT for the quantum standard map: a paradigmatic example of a kicked quantum system. Moreover, we show that finite-size precursors of ESQPTs shrink as chaos increases due to the disturbance of the system. This phenomenon is explained through destructive interference between principal homoclinic orbits.

DOI: 10.1103/PhysRevE.104.L062202

Critical phenomena are ubiquitous in physics. They are characterized by nonanalyticities of measurable observables and have a profound impact on several aspects of the statistical and dynamical properties of physical systems [1]. In quantum mechanics, criticality can manifest itself in individual states due to the discreteness of the spectrum. For instance, at zero temperature, a quantum phase transition is expressed by an abrupt change in the ground state when a parameter is varied [2]. When this occurs for excited states, it is called excited-state quantum phase transition (ESQPT) [3]. It appears when the level density reveals singularities that have important consequences in the collective behavior of interacting many-body systems [3]. It also has effects on decoherence [4,5], quantum thermodynamics [6,7], quantum information [8], and condensate physics [9,10].

ESQPTs have been studied in autonomous and periodically driven systems. In the latter, criticality appears in quasienergy states, which are a direct generalization of ESQPTs for driven quantum systems [11–13]. The Floquet map represents the collective variables of a many-body system. In general ESQPTs have been related to phase space structures associated with the classical limit of the system [3]. In classical integrable systems, unstable periodic orbits and their manifolds make up the separatrices that divide classical phase space into disjoint areas of regular motion. Moreover, they are sensitive to disturbances, giving rise to chaotic regions when the system is perturbed; that is, their breakdown generates homoclinic and heteroclinic tangles which are the originating causes of chaos [14]. Although some consequences of the destruction of these structures have been studied in connection with ESQPT [3,15–20], the main aspects of this process have yet to be understood.

Semiclassical theories have been the bridge between the classical and quantum worlds and have had extraordinary success in explaining various phenomena [21]. For integrable or strongly chaotic motions, semiclassical theories are much more developed [22] than in the case of nearly integrable or mixed dynamics, where islands of stability coexist with chaotic layers [23]. At the same time, ESQPTs have been described using semiclassical torus quantization near a separatrix, but this technique works for integrable systems but fails when chaos appears. In this case the separatrix associated with the unstable periodic orbit (PO) breaks, and new invariant structures which are robust with respect to perturbations emerge: the stable and unstable manifolds. Recently, a semiclassical theory of wave propagation based on stable and unstable manifolds of unstable POs was developed [24–26]. This method has been proven to be very efficient for the calculation of high energy levels of strongly chaotic systems [27], but it has yet to be tested (used) in the mixed regime.

In this Letter we use this state-of-the-art semiclassical method to show that the advent of chaos in the classical model can result in the weakening of finite-size precursors of ESQPTs. We find a simple semiclassical criterion specifying the transition from the finite-size manifestation of quantum criticality to quantum chaos. We predict when this effect occurs depending on the size of the disturbance that changes the ratio between a canonical invariant of the principal homoclinic orbits and the Planck constant in our model (or the inverse of the number of particles in many-body systems). The decrease of finite-size precursors of ESQPTs is produced by the interference of principal homoclinic orbits, giving rise to scarred states—i.e., states with accumulated probability density—on satellite POs related to the homoclinic motion [28,29].

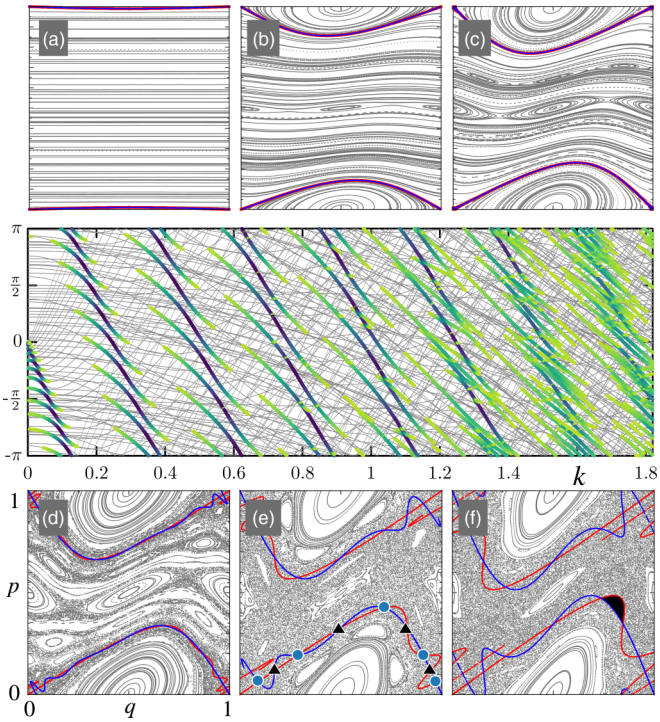

FIG. 1. (a)–(f) Classical phase space for the standard map for $k = 0.001$, 0.2, 0.5, 1, 1.5, and 1.8, showing the stable (blue/dark gray printed, line) and unstable (red/light gray printed, line) manifolds of z_0. (e) displays the first (circles) and second (triangles) homoclinic orbits of z_0. (f) shows a black area indicating the invariant ΔS. The middle panel shows a correlation diagram for the eigenphases of the quantized standard map with $N = 158$ as a function of the perturbation parameter k; high intensities $|c_i|^2 > 5 \times 10^{-3}$ are plotted in color. Darker shade corresponds to larger $|c_i|^2$.

For our calculations we have used a map that stems from a periodically kicked Hamiltonian, the paradigmatic standard map [30]. However, it is important to highlight that the conclusions reached have general validity. The standard map is a two-dimensional area-preserving map depending on a perturbation parameter k. This map evolves point $z = (q, p)$ in the unit torus to point $z' = (q', p')$ by the following rule:

$$p' = p + \frac{k}{2\pi}\sin(2\pi q), \quad \mathrm{mod}\,1$$
$$q' = p' + q, \quad \mathrm{mod}\,1. \tag{1}$$

This map is generated by the time-dependent Hamiltonian $H(q, p, t) = p^2/2 + k/(2\pi)^2 \cos(2\pi q) \sum \delta(t - n)$. For small $k \approx 0$ the map is almost integrable, and as k increases, invariant tori begin to break. For very large k there are no visible regular islands (although small ones do appear for certain values); Fig. 1 shows phase portraits for $k = 0.001, 0.2, 0.5, 1$, 1.5, and 1.8. Upon quantization the map is a unitary operator that can be expressed as a product of two kicks,

$$\hat{U} = \exp\left(-i\frac{\hat{p}^2}{2\hbar}\right)\exp\left(-i\frac{k}{\hbar}\cos(2\pi\hat{q})\right). \tag{2}$$

The phase space topology implies a finite Hilbert space of dimension N and effective Planck constant $\hbar = 1/(2\pi N)$. Therefore, $\hat{U}$ is represented by an $N \times N$ matrix, and after diagonalization, we analyze spectral properties in terms of the set of eigenphases ϕ_i corresponding to the eigenstates $\hat{U}\,|\phi_i\rangle = e^{i\phi_i}\,|\phi_i\rangle$. We emphasize that the parameter N corresponds to the particle number in a many-body system [11].

We now consider precursors of critical behavior in the quasienergy spectrum associated with the separatrix generated by the unstable PO of period 1 at $z_0 = (0, 0)$. Such an invariant structure is broken even for an arbitrarily small perturbation, and then a chaotic layer dominated by the stable and unstable manifolds of z_0 emerges [see Figs. 1(a)–1(f)]. In order to study eigenfunctions localized on invariant curves influenced by z_0, we compute $|z_0\rangle = \sum c_i\,|\phi_i\rangle$, with $|z_0\rangle$ being a suitable normalized wave packet centered at z_0. This wave packet is the map version of a Gaussian beam construction on unstable POs, named the resonance of the PO [31] (see the Supplemental Material [32]).

In Fig. 1 (central frame) we show the eigenphases as a function of the perturbation k (gray lines) for $N = 158$. The thick colored lines mark eigenstates with high (darker shade) intensity $|c_i|^2$. One clearly sees the emergence of an ES-QPT precursor spectral structure in the form of Demkov-type avoided level crossings [33,34] that follows the states with the greatest overlap with the resonance of z_0 (darker shade in Fig. 1). This structure follows a straight line, which can be identified with the Bohr-Sommerfeld (BS) phase ϕ_{BS}. The BS phase of $|z_0\rangle$ is a semiclassical estimate for the phase of the matrix element $\langle z_0|\hat{U}|z_0\rangle$, resulting in [35]

$$\phi_{\mathrm{BS}} = \left(-\frac{kN}{2\pi}\right)_{\mathrm{mod}(2\pi)} \simeq \sum |c_i|^2 \tilde{\phi}_i, \tag{3}$$

and the corresponding phase dispersion is given by $\sigma_\phi = \lambda/\sqrt{2} \simeq [\sum |c_i|^2(\tilde{\phi}_i - \phi_{\mathrm{BS}})^2]^{1/2}$, with $\lambda = \ln(1 + k/2 + \sqrt{k + k^2/4})$ being the stability exponent of z_0. Here $\tilde{\phi}_i$ is just ϕ_i or $\phi_i \pm 2\pi$; one selects the value that minimizes $(\tilde{\phi}_i - \phi_{\mathrm{BS}})^2$. This nonisolated avoided crossing structure is observed in several models of many-body systems [3]. It can also be observed in the elliptic billiard [34] and molecular systems [33,36]. Figure 1 also shows that as the perturbation grows, this structure gradually disappears, and for $k \gtrsim 1.4$ it is difficult to observe the sequence of Demkov avoided crossings. Understanding the physical process involved in the destruction of this structure is the most important achievement of this Letter. We emphasize that the expressions obtained for ϕ_{BS} and σ_ϕ depend on only the properties of the neighborhood of z_0 because they are associated with the short time dynamics up to the Ehrenfest time. Nevertheless, later we will compute the inverse participation ratio of the intensities $|c_i|^2$, which depends on the long time dynamics up to the Heisenberg time, and then as we will show, a clear transition to quantum chaos will be appreciated.

To understand the mechanism associated with the avoided crossings we first notice that for a small perturbation, the separatrix divides the phase space into two regions where the motion is a rotation or a libration, just like in a planar pendulum. Then, as we move adiabatically on an eigenphase with high intensity that passes through an avoided crossing, the corresponding eigenstate, previously localized on an invariant

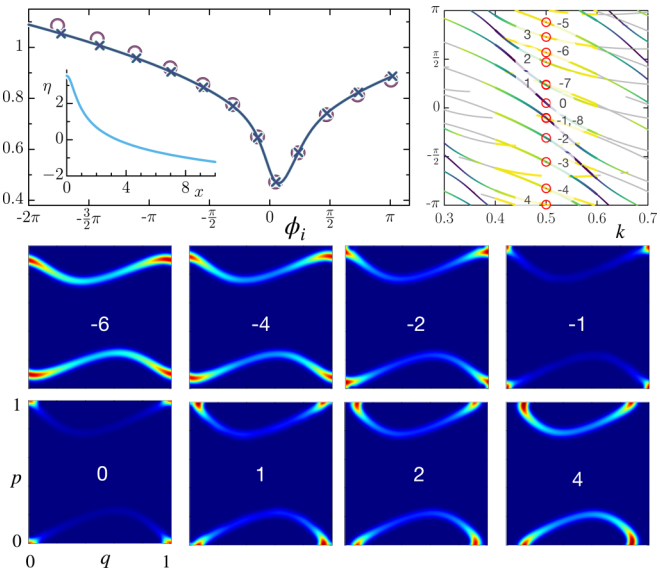

FIG. 2. Manifestation of ESQPT in the eigenphase spectrum of the standard map. Top left: Difference $\phi_{i+1} - \phi_i$ vs ϕ_i for $k = 0.5$ and $N = 158$. Circles and crosses indicate quantum and semiclassical calculations, respectively. The inset shows $\eta(x)$ of Eq. (4). Top right: Correlation diagram for $N = 158$ in the range $k = (0.3, 0.7)$. The thick colored lines represent $|c_i|^2 > 5 \times 10^{-6}$. Bottom: Several eigenstates of the ESQPT in the Hussimi representation.

curve corresponding to rotation, transitions to an invariant curve that corresponds to libration [32].

Let us discuss the structure of eigenfunctions and eigenphases with the highest intensities $|c_i|^2$ at $k = 0.5$, a value of perturbation far from the breakup region (see Fig. 1). In the top right panel of Fig. 2 the eigenphases with the highest $|c_i|^2$ are marked with red circles, while in the top left panel we show the neighbor spacings $\phi_{i+1} - \phi_i$ vs ϕ_i. These spacings have a minimum at $\phi_{\rm BS}$, with this bunching of levels being a characteristic feature for ESQPT; that is, quantum criticality is expressed by the accumulation of levels around the separatrix [8]. To compute the spacings the phases need to be unfolded; that is, if ϕ_i is in a line coming from a previous (subsequent) Demkov structure, we add (subtract) 2π. The corresponding eigenfunctions are localized on invariant tori close to the separatrix; the bottom panels of Fig. 2 display the Husimi function [37] of these states. The state closest to the separatrix, labeled 0, is highly localized on the periodic point z_0 due to the dynamics on the separatrix. States labeled with positive integers are localized on tori with libration motion, and those labeled with negative integers are on tori with rotation motion.

Now we will obtain the previous result at a semiclassical level by using a technique based on the stable and unstable manifolds of z_0 (thick red and blue lines in Fig. 1). The intersection of these manifolds defines the set of homoclinic orbits (HOs) of z_0. Each HO consists of an infinite sequence of points that accumulate at z_0. The main accomplishment of this theory is the ability to compute a semiclassical autocorrelation function of the wave packet centered on a PO, which is written as a sum over HOs, each one characterized by four canonical invariants (see [27,32] for more details). Then, the Fourier transform of the autocorrelation function gives a smoothing of the spectral function $\Phi(\phi) = \sum |c_i|^2 \delta(\phi - \tilde{\phi}_i)$, expressed in terms of the product of two real functions $\tilde{F}(\phi)\Sigma(\phi)$ [32]. The function $\tilde{F}(\phi)$ is positive definite and describes the envelope of the intensities, with a maximum value at $\phi = \phi_{\rm BS}$. As we are interested here only in the semiclassical determination of $\tilde{\phi}_i$, this function is not relevant for our analysis. In contrast, the function $\Sigma(\phi)$ is strongly oscillatory, and its maxima give us the eigenphases influenced by $|z_0\rangle$. This function is a sum over HOs, where each term is the product of an amplitude and the cosine of the phase [27],

$$\psi_j(\phi) = S_j/\hbar - \mu_j \pi/2 + x\eta(x) + x \ln(A_j/\hbar), \qquad (4)$$

where $x = (\phi_{\rm BS} - \phi)/\lambda$, S_j is the homoclinic action, μ_j is the homoclinic Maslov index, and A_j is the relevance. Moreover, $\eta(x)$ is a real even function with the only maximum at the origin (see the inset in the top left panel of Fig. 2 and further details in [32]). The evolution up to the Heisenberg time requires an enormous number of terms in the sum of $\Sigma(\phi)$. Nevertheless, we want to describe eigenfunctions localized on invariant curves close to the broken separatrix, which are well defined in terms of an evolution up to the Ehrenfest time. Therefore, only a few HOs are sufficient. Using a large number of HOs in this case does not provide new information, and the only effect is to reduce the width of the smoothed delta functions defining the eigenphases. Furthermore, for small and moderated perturbations the amplitudes associated with the first two HOs are much greater than the next ones, and consequently, we will restrict the analysis to these two. These amplitudes are very similar in the considered range of k; e.g., the relative difference is 3.9×10^{-5} for $k = 0.5$ and goes to zero with k. Then to evaluate the maxima of $\Sigma(\phi)$ we include only the cosine factors $\Sigma(\phi) \propto \cos(\psi_1) + \cos(\psi_2)$. To compute this function we notice that the first HO is marked with circles in Fig. 1(e), and the second one is marked with triangles. The homoclinic Maslov indices are $\mu_1 = 0$ and $\mu_2 = 1$ for all k. For $k = 0.5$, $S = (S_1 + S_2)/2 \approx 0.142258$, $\Delta S = S_2 - S_1 \approx 1.2 \times 10^{-5}$, $A = (A_1 + A_2)/2 \approx 0.53998$, and $\Delta A = A_2 - A_1 \approx 5.8 \times 10^{-4}$.

We express $\cos(\psi_1) + \cos(\psi_2) = 2\cos(\psi)\cos(\Delta\psi/2)$, with $\psi = (\psi_1 + \psi_2)/2$ and $\Delta\psi = \psi_2 - \psi_1$. To leading order in the small quantity $\epsilon = \Delta A/A$ (ϵ goes to zero with k) we can consider $\Delta\psi = \Delta S/\hbar - \pi/2 + O(\epsilon)$ to be a constant (independent of ϕ). Hence, the maxima of the sum of cosines can be found (to leading order) with the quantization condition ($\cos\psi = 1$)

$$\psi = S/\hbar - \pi/4 + x\eta(x) + x \ln(A/\hbar) = 2\pi n. \qquad (5)$$

This condition for finding the eigenphases that participate in the ESQPT is important because it associates each solution with the quantum number n, an essential ingredient when the perturbation goes to zero. The integer providing the eigenphase with the smallest $|x|$ is $n_0 = 22$, corresponding to the one labeled 0 in Fig. 2, and the solution with $n = n_0 - l$ is the eigenphase labeled l. The top left panel of Fig. 2 shows that quantum and semiclassical calculations are very close. Furthermore, we have verified the accuracy of the eigenphases obtained from Eq. (5) for N up to 3000, finding an error $O(1/N)$. However, below we show that there is a critical value of N after which the validity of Eq. (5) no

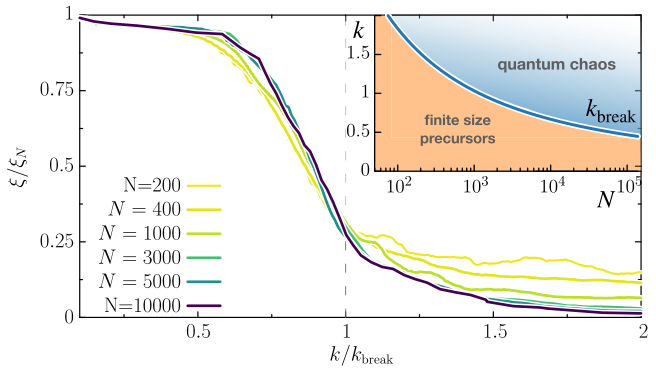

FIG. 3. Normalized running average of the IPR of $|z_0\rangle$ vs $k/k_{\rm break}$ for $N = 200$, 400, 1000, 3000, 5000, and 10 000. For all the curves a running average was performed to smooth out the fluctuations. Inset: $k_{\rm break}$ vs N (see text for details). The normalization factor was empirically found to behave as $\xi_N \approx 3/(3.75 + \ln N)$.

longer holds. Finally, we notice that an estimate of the mean nearest-neighbor spacing for the solutions of Eq. (5) is given by $\Delta\phi \sim \lambda/\ln(A/\hbar)$. Then, the number of eigenstates influenced by $|z_0\rangle$ results in $2\sigma_\phi/\Delta\phi \propto \ln(A/\hbar)$, and consequently, the phenomenon of ESQPT introduces a logarithmic divergence for the mean density of states at $\phi_{\rm BS}$ in the semiclassical limit.

The quantization condition of Eq. (5) works over a wide range of perturbations up to $k \approx 1.1$ for the $N = 158$ case considered in Figs. 1 (central panel) and 2. Even though throughout this transition the chaotic region is (classically) growing, it is not large enough to be detected by quantum mechanics. This is evidence that the existence of classical chaos does not necessarily affect fine-size precursors. For larger k it is difficult to associate semiclassical solutions with quantum eigenphases, and for $k \approx 1.6$ the finite-size manifestation of ESQPT is destroyed. Due to the fact that this structure mainly depends on the first two HOs, it is expected that the destruction of the precursor of ESQPT happens when the contributions of these HOs cancel each other out. This criterion of strong perturbation occurs for $\cos(\Delta\psi/2) = 0$, or, equivalently, for $\Delta S/\hbar = 3\pi/2$. The functional dependence of ΔS on k allows us to define a perturbation value $k_{\rm break}$ where the ESQTP breaks up. Based on the definition of ΔS [see shaded area in Fig. 1(f)], we have obtained the following expression [32]:

$$\Delta S(k) \approx 6\pi\left(1 - 0.341k^{1/3}\right)\exp\left(-\frac{\pi^2}{\sqrt{k}}\right), \qquad (6)$$

with the exponential factor extracted from Ref. [38]. We observe that a characteristic of the breakup region is a sudden proliferation of contributing eigenphases. This effect is detected by a measure of localization of $|z_0\rangle$ in the basis $|\phi_i\rangle$ such as the inverse participation ratio $\xi = \sum |c_i|^4$. In Fig. 3 we show ξ/ξ_N, where ξ_N is a normalization factor so that $\xi/\xi_N = 1$ for $k \to 0$, as a function of the renormalized perturbation $k/k_{\rm break}$ for several values of N [32]. The evidence of full delocalization for $k/k_{\rm break} \approx 1$ supports the accuracy of our ESQPT breakup estimation. In the inset of Fig. 3 we show $k_{\rm break}$ as a function of N, which defines a phase diagram

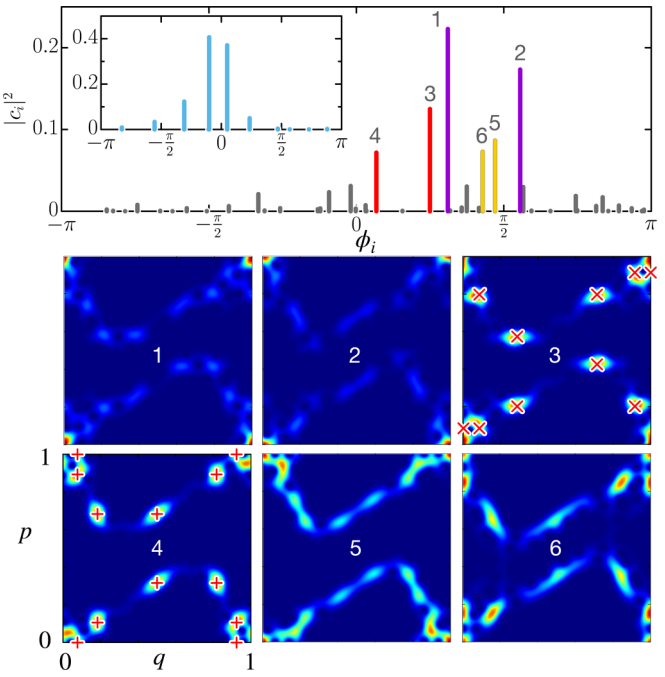

FIG. 4. Top: Intensities $|c_i|^2$ of $|z_0\rangle$ for $k = 1.447$ and $N = 158$; the inset shows the case $k = 0.5$ and $N = 158$. Bottom: Husimi representation of eigenstates with high intensities. Panel 3 shows a satellite PO (crosses) of the first HO, and panel 4 shows a satellite PO (pluses) of the second HO.

showing a region in which traces of ESQPT remain and a region where the precursors of criticality are fully destroyed. It can be clearly seen that $k_{\rm break}$ goes to zero in the semiclassical limit ($N \to \infty$).

Let us finally discuss qualitatively the transition process from localization to delocalization for $|z_0\rangle$. The top panel of Fig. 4 displays $|c_i|^2$ for $N = 158$ and $k = 1.447$ close to $k_{\rm break}(158) \approx 1.62$, showing a much more complicated systematic than the intensities for $k = 0.5$ (shown in the inset). Intensities 1 and 2 are predicted for consecutive solutions of Eq. (5) with $n = 37$ and $n = 38$, respectively, while the associated states are reminiscent of states 0 and -1 in Fig. 2. The intensity labeled 3 approximately satisfies the equation $\psi_1 = 2\pi n_1$, with $n_1 = 38$, and state 3 shows a strong scar [27] of the PO, displayed by crosses; this PO is a satellite PO of the first HO [39]. Equivalently, intensity 4 verifies the equation $\psi_2 = 2\pi n_2$, with $n_2 = 39$, and state 4 shows a strong scar of the PO, displayed by pluses, which is a satellite of the second HO. Finally, intensities 5 and 6 are not close to any of the three equations mentioned before, and both states exhibit characteristics of the three structures discussed in the previous panels. This description suggests that for k close to $k_{\rm break}$, the phenomenon of scarring manifests clearly on satellite POs of the principal HOs, providing a signature of chaos at the quantum level. One observes a competition between two processes: coherent interference between HOs in order to generate ESQPT states and destructive interference between HOs giving rise to scars of satellite POs.

In summary, the effect of a perturbation on the finite-size precursors of ESQPTs was analyzed. We have demonstrated that the advent of chaos can decrease the quantum

manifestations of an ESQPT whenever quantum mechanics is able to detect the small scale structures generated by chaos. In this sense classical chaos is a necessary but not sufficient condition to affect finite-size precursors of ESQPT. We revealed that the mechanism of this phenomenon is the destructive interference between principal homoclinic orbits of the unstable periodic trajectory that generates criticality. Moreover, a semiclassical criterion specifying a transition to quantum chaos was established. Finally, we would like to emphasize the use of manifolds of unstable POs for the semiclassical description of a quantum perturbation. These Lagrangian manifolds, unlike tori, are structurally stable and for this reason are suitable for analyzing the effect of perturbations over the system.

We acknowledge the valuable discussions held with J. Diego Urbina and Q. Hummel. The work was partially supported by CONICET (PIP 112201 50100493CO), UBACyT (Grant No. 20020170100234BA), ANPCyT (PICT-2016-1056). I.G.-M. received support from the French-Argentinian project LIA-LICOQ.

[1] P. Coleman and A. Schofield, Quantum criticality, Nature (London) **433**, 226 (2005).

[2] S. Sachdev, *Quantum Phase Transitions* (Cambridge University Press, Cambridge, 1999).

[3] P. Cejnar, P. Stránský, M. Macek, and M. Kloc, Excited-state quantum phase transitions, J. Phys. A **54**, 133001 (2021).

[4] A. Relaño, J. M. Arias, J. Dukelsky, J. E. García-Ramos, and P. Pérez-Fernández, Decoherence as a signature of an excited-state quantum phase transition, Phys. Rev. A **78**, 060102(R) (2008).

[5] Q. Wang and F. Pérez-Bernal, Excited-state quantum phase transition and the quantum-speed-limit time, Phys. Rev. A **100**, 022118 (2019).

[6] Q. Wang and H. T. Quan, Probing the excited-state quantum phase transition through statistics of Loschmidt echo and quantum work, Phys. Rev. E **96**, 032142 (2017).

[7] Q. Wang and F. Pérez-Bernal, Characterizing the Lipkin-Meshkov-Glick model excited-state quantum phase transition using dynamical and statistical properties of the diagonal entropy, Phys. Rev. E **103**, 032109 (2021).

[8] Q. Hummel, B. Geiger, J. D. Urbina, and K. Richter, Reversible Quantum Information Spreading in Many-Body Systems near Criticality, Phys. Rev. Lett. **123**, 160401 (2019).

[9] T. Tian, H.-X. Yang, L.-Y. Qiu, H.-Y. Liang, Y.-B. Yang, Y. Xu, and L.-M. Duan, Observation of Dynamical Quantum Phase Transitions with Correspondence in an Excited State Phase Diagram, Phys. Rev. Lett. **124**, 043001 (2020).

[10] P. Feldmann, C. Klempt, A. Smerzi, L. Santos, and M. Gessner, Interferometric Order Parameter for Excited-State Quantum Phase Transitions in Bose-Einstein Condensates, Phys. Rev. Lett. **126**, 230602 (2021).

[11] V. M. Bastidas, G. Engelhardt, P. Pérez-Fernández, M. Vogl, and T. Brandes, Critical quasienergy states in driven many-body systems, Phys. Rev. A **90**, 063628 (2014).

[12] V. M. Bastidas, P. Pérez-Fernández, M. Vogl, and T. Brandes, Quantum Criticality and Dynamical Instability in the Kicked-Top Model, Phys. Rev. Lett. **112**, 140408 (2014).

[13] J. N. Bandyopadhyay and T. Guha Sarkar, Effective time-independent analysis for quantum kicked systems, Phys. Rev. E **91**, 032923 (2015).

[14] M. A. Lieberman and A. J. Lichtenberg, *Regular and Stochastic Motion*, 2nd ed., Applied Mathematical Sciences (Springer, New York, 1983), Vol. 38.

[15] M. Kloc, P. Stránský, and P. Cejnar, Quantum quench dynamics in Dicke superradiance models, Phys. Rev. A **98**, 013836 (2018).

[16] P. Stránský, M. Macek, and P. Cejnar, Excited-state quantum phase transitions in systems with two degrees of freedom: Level density, level dynamics, thermal properties, Ann. Phys. (NY) **345**, 73 (2014).

[17] P. Stránský, M. Macek, A. Leviatan, and P. Cejnar, Excited-state quantum phase transitions in systems with two degrees of freedom: II. Finite-size effects, Ann. Phys. (NY) **356**, 57 (2015).

[18] M. Macek, P. Stránský, A. Leviatan, and P. Cejnar, Excited-state quantum phase transitions in systems with two degrees of freedom. III. Interacting boson systems, Phys. Rev.C **99**, 064323 (2019).

[19] M. Kloc, P. Stránský, and P. Cejnar, Monodromy in Dicke superradiance, J. Phys. A **50**, 315205 (2017).

[20] M. Kloc, P. Stránský, and P. Cejnar, Quantum phases and entanglement properties of an extended Dicke model, Ann. Phys. (NY) **382**, 85 (2017).

[21] M. Brack and R. Bhaduri, *Semiclassical Physics* (Addison-Wesley, California, 1997).

[22] M. C. Gutzwiller, *Chaos in Classical and Quantum Mechanics*, Interdisciplinary Applied Mathematics (Springer, New York, 2013).

[23] I. C. Percival, Chaos in Hamiltonian systems, *Dynamical Chaos*, edited by M. V. Berry, I. C. Percival, and N. O. Weiss (Princeton University Press, 2014), pp. 131–144.

[24] E. G. Vergini, Semiclassical Approach to Long Time Propagation in Quantum Chaos: Predicting Scars, Phys. Rev. Lett. **108**, 264101 (2012).

[25] E. G. Vergini, Semiclassical propagation up to the Heisenberg time, Europhys. Lett. **103**, 20003 (2013).

[26] E. G. Vergini, Semiclassical theory of long time propagation in quantum chaos. First part, J. Phys. A **53**, 395703 (2020).

[27] E. G. Vergini, Semiclassical quantization of highly excited scar states, Europhys. Lett. **118**, 10005 (2017).

[28] D. Wisniacki, E. Vergini, R. Benito, and F. Borondo, Signatures of Homoclinic Motion in Quantum Chaos, Phys. Rev. Lett. **94**, 054101 (2005).

[29] D. A. Wisniacki, E. Vergini, R. M. Benito, and F. Borondo, Scarring by Homoclinic and Heteroclinic Orbits, Phys. Rev. Lett. **97**, 094101 (2006).

[30] B. Chirikov and D. Shepelyansky, Chirikov standard map, Scholarpedia **3**, 3550 (2008).

[31] E. G. Vergini and G. G. Carlo, Semiclassical construction of resonances with hyperbolic structure: The scar function, J. Phys. A **34**, 4525 (2001).

[32] See Supplemental Material at http://link.aps.org/supplemental/10.1103/PhysRevE.104.L062202 where we provide more details about the evolution of eigenstates on the ESQPT, the

semiclassical construction of a resonance at a given fixed point the the smoothing of its spectral decomposition. In addition further details are provided that aid the comprehension of the main text, like the scaling of the participation ratio with the system size and more complementary data, which includes Refs. [26,27].

[33] F. J. Arranz, F. Borondo, and R. M. Benito, Avoided crossings, scars, and transition to chaos, J. Chem. Phys. **107**, 2395 (1997).

[34] J.-H. Kim, J. Kim, C.-H. Yi, H.-H. Yu, J.-W. Lee, and C.-M. Kim, Avoided level crossings in an elliptic billiard, Phys. Rev. E **96**, 042205 (2017).

[35] D. Schneider, E. G. Vergini, and A. M. F. Rivas, The short periodic orbit approach for the quantum cat maps, J. Phys. A **41**, 405102 (2008).

[36] F. J. Arranz, F. Borondo, and R. M. Benito, Scar Formation at the Edge of the Chaotic Region, Phys. Rev. Lett. **80**, 944 (1998).

[37] K. Husimi, Some formal properties of the density matrix, Nippon Sugaku-Buturigakkwai Kizi Dai 3 Ki **22**, 264 (1940).

[38] V. F. Lazutkin, I. G. Schachmannski, and M. B. Tabanov, Splitting of separatrices for standard and semistandard mappings, Phys. D (Amsterdam, Neth.) **40**, 235 (1989).

[39] Associated with each HO, there is an infinite set of unstable satellite POs which approximate the motion of the HO more and more as the period goes to infinity. Furthermore, the Bohr-Sommerfeld phase of these satellite POs is close to the quantization of the HO expressed by the relationship $\psi_j = 2\pi n$.